

Dominant-negative inhibition of the Axl receptor tyrosine kinase suppresses brain tumor cell growth and invasion and prolongs survival

Peter Vajkoczy^{*†}, Pjotr Knyazev[‡], Andrea Kunkel^{*}, Hans-Holger Capelle^{*}, Sandra Behrndt^{*}, Hendrik von Tengg-Kobligk[§], Fabian Kiessling[¶], Uta Eichelsbacher[‡], Marco Essig[§], Tracy-Ann Read^{||}, Ralf Erber^{*}, and Axel Ullrich^{**}

^{*}Department of Neurosurgery, Medical Faculty of the University of Heidelberg, D-68167 Mannheim, Germany; [§]Department of Radiology and [¶]Department of Medical Physics in Radiology, German Cancer Research Center, D-69120 Heidelberg, Germany; [‡]Department of Molecular Biology, Max Planck Institute for Biochemistry, D-82152 Martinsried, Germany; ^{||}Department of Anatomy and Cell Biology, University of Bergen, N-5020 Bergen, Norway; and ^{**}Center of Molecular Medicine, Institute of Molecular and Cell Biology, Singapore 138673

Communicated by Erkki Ruoslahti, The Burnham Institute, La Jolla, CA, January 9, 2006 (received for review August 15, 2005)

Malignant gliomas remain incurable brain tumors because of their diffuse-invasive growth. So far, the genetic and molecular events underlying gliomagenesis are poorly understood. In this study, we have identified the receptor tyrosine kinase Axl as a mediator of glioma growth and invasion. We demonstrate that Axl and its ligand Gas6 are overexpressed in human glioma cell lines and that Axl is activated under baseline conditions. Furthermore, Axl is expressed at high levels in human malignant glioma. Inhibition of Axl signaling by overexpression of a dominant-negative receptor mutant (AXL-DN) suppressed experimental gliomagenesis (growth inhibition >85%, $P < 0.05$) and resulted in long-term survival of mice after intracerebral glioma cell implantation when compared with Axl wild-type (AXL-WT) transfected tumor cells (survival times: AXL-WT, 10 days; AXL-DN, >72 days). A detailed analysis of the distinct hallmarks of glioma pathology, such as cell proliferation, migration, and invasion and tumor angiogenesis, revealed that inhibition of Axl signaling interfered with cell proliferation (inhibition 30% versus AXL-WT), glioma cell migration (inhibition 90% versus mock and AXL-WT, $P < 0.05$), and invasion (inhibition 62% and 79% versus mock and AXL-WT, respectively; $P < 0.05$). This study describes the identification, functional manipulation, *in vitro* and *in vivo* validation, and preclinical therapeutic inhibition of a target receptor tyrosine kinase mediating glioma growth and invasion. Our findings implicate Axl in gliomagenesis and validate it as a promising target for the development of approaches toward a therapy of these highly aggressive but, as yet, therapy-refractory, tumors.

angiogenesis | glioma | metastasis | protooncogene | signaling

Malignant gliomas are the most common and most aggressive brain tumors because of their highly invasive growth (1, 2). Understanding the mechanisms of gliomagenesis and glioma invasion is essential to developing new therapeutic strategies. However, the underlying genetic and molecular events have remained obscure so far (reviewed in ref. 3). Receptor tyrosine kinases (RTKs) represent regulatory proteins that play an important role in growth and differentiation of normal cells. Moreover, RTKs represent a major class of protooncogenes, involved in the progression and metastasis of cancer cells (4). As a result, several RTKs are being actively pursued as targets for therapeutic intervention.

The Axl receptor is a RTK originally identified as a transforming gene in chronic myeloid leukemia (5, 6). Axl is characterized by a unique molecular structure, in that the intracellular region has the typical structure of a RTK, and the extracellular domain contains fibronectin III and Ig motifs similar to cadherin-type adhesion molecules. During development, Axl is expressed in various organs, including the brain, suggesting that this RTK is involved in mesenchymal and neural development (7, 8). In the adult, Axl expression is low (9) but returns to high expression levels in a variety of

tumors (10–13). Gas6 is, so far, the single, activating ligand for Axl (14). Moreover, additional ligand-independent mechanisms may exist by which Axl functions, such as signaling through homophilic interactions (15). Rather than conferring a mitogenic signal, Axl has been suggested to be involved in cell survival, cellular adhesion, and chemotaxis as well as blood vessel function (15–19). Because its expression correlates with the metastatic potential of neoplasms, Axl may also play a role during invasion. Thus, Axl behaves as an oncoprotein when it is overexpressed, but its mechanisms of action have not been understood so far.

Here, we demonstrate that Axl is highly expressed and activated in human glioma cell lines and human malignant glioma specimens. Experimental inhibition of Axl signaling suppressed glioma growth and prolonged survival in nude mice. Our results indicate a role for Axl in mediating glioma cell proliferation and glioma cell migration/invasion. Specific targeting of Axl may represent a promising approach to intervene with cancer progression and recurrence.

Results

Expression and Activation of Axl in Cells of Malignant Glioma. We have initially profiled RTKs in malignant glioma cell lines by using a tyrosine kinase-based cDNA array (20) and found high expression levels for Axl mRNA in the majority of the tested cell lines (data not shown). Expression of Axl in human glioma cell lines was reassessed by using an advanced array containing 645 genes, including encoded protein kinases, protein phosphatases, and other signaling proteins (Fig. 1A). Here, a >2-fold up-regulation of Axl mRNA expression was observed in seven of nine glioma cell lines tested (bars 1–9, Fig. 1A). Interestingly, Axl mRNA expression levels were not elevated in nonglial, neoplastic cell lines, i.e., three neuroblastoma cell lines (JMR32, SKSNH, and SHSY5Y) and one medulloblastoma cell line (TE671) (bars 10–13, Fig. 1A). The result obtained from the array analysis was confirmed by Northern analysis (Fig. 1B). Because Axl activation in tumor cells has been suggested to follow an autocrine/paracrine pathway (21), we next addressed the expression of the Axl ligand Gas6 in cell lines displaying the corresponding receptor. Northern blot analysis revealed positivity for Gas6 expression in all tumor cell lines tested, demonstrating coordinated expression of Axl and Gas6 mRNA in the majority of glioma cell lines (Fig. 1B). Next, expression of Axl

Conflict of interest statement: P.V., P.K., and A.U. have filed a patent on the role of Axl in tumor biology. The patent has been licensed by the company U3, which pursues Axl as a potential target for antitumor therapy.

Abbreviation: RTK, receptor tyrosine kinase.

[†]To whom correspondence should be addressed at: Department of Neurosurgery, Klinikum Mannheim, University of Heidelberg, Theodor-Kutzer-Ufer 1-3, D-68167 Mannheim, Germany. E-mail: peter.vajkoczy@nch.ma.uni-heidelberg.de.

© 2006 by The National Academy of Sciences of the USA

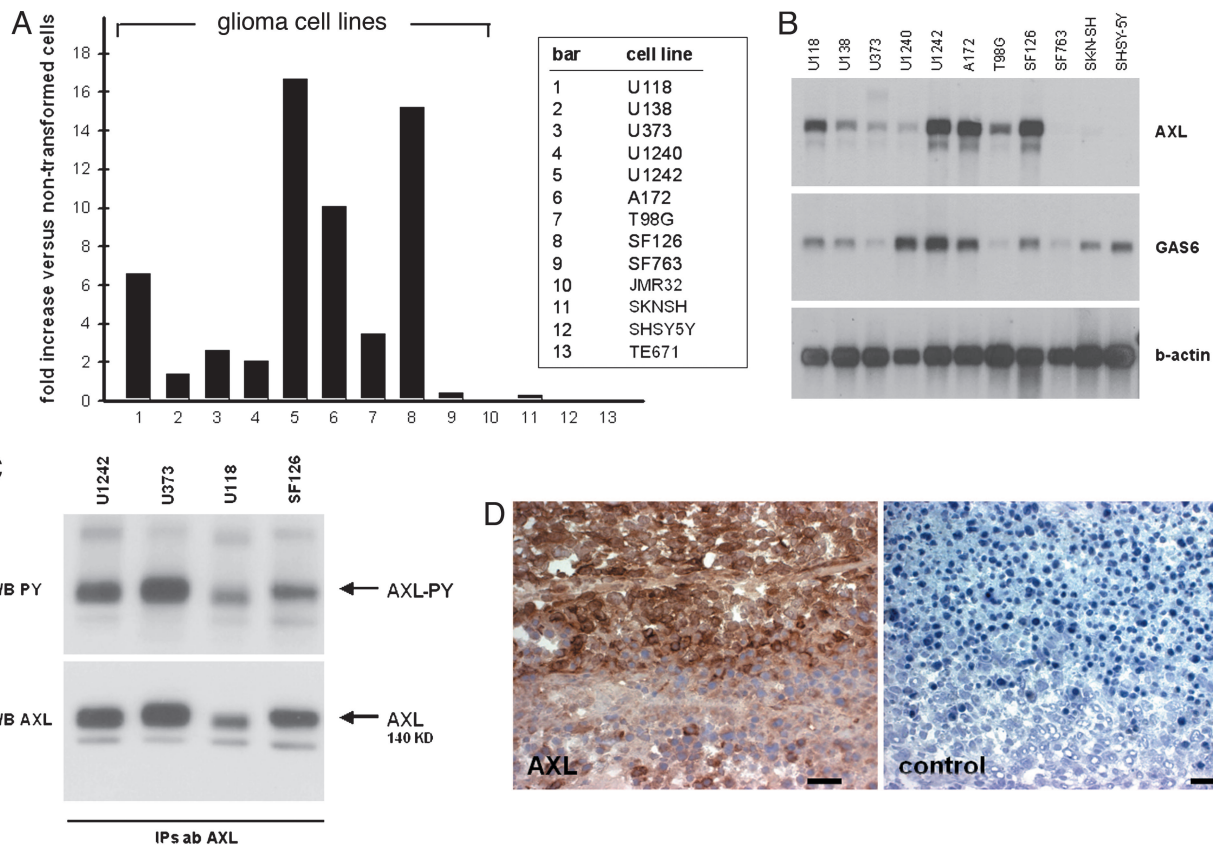


Fig. 1. Expression of Axl in malignant glioma cells. (A) Relative expression level of Axl mRNA in human glioma cell lines (bars 1–9), neuroblastoma cell lines (bars 10–12), and a medulloblastoma cell line (bar 13) versus the nonneoplastic cell line HCN2 as assessed by cDNA array analysis. (B) Northern blot analysis of Axl and Gas6. Total RNA was isolated from human glioma cell lines and neuroblastoma cell lines. A β -actin probe was used as internal control. (C) Western blot analysis for Axl protein (WB AXL, Lower) and phosphotyrosine (WB PY, Upper) after immunoprecipitation of Axl protein. Cellular protein was isolated from four human glioma cell lines. (D) Immunohistochemical staining of Axl protein in a human glioblastoma multiforme specimen. Negative control staining was performed in the absence of the primary antibody. (Scale bar, 50 μ m.)

protein was addressed in four glioma cell lines: U1242, U373, U118, and SF126. Western blotting of the lysate revealed a 140-kDa protein corresponding to the full-length Axl receptor as well as a 120-kDa protein corresponding to the smaller precursor for the full-length protein (22). Immunoprecipitation of cell lysates using the Axl-specific antibody and probing with an anti-phosphotyrosine antibody demonstrated high baseline phosphorylation levels of Axl

in all glioma cell lines (Fig. 1C). Finally, we analyzed human glioblastoma multiforme specimens. As demonstrated in Fig. 1D, immunohistochemical staining with the anti-Axl antibody revealed abundant Axl protein expression in tumor cells.

Inhibition of Axl Signaling Inhibits Experimental Tumor Growth. Next, we addressed the role of Axl for glioma biology, choosing SF126 as

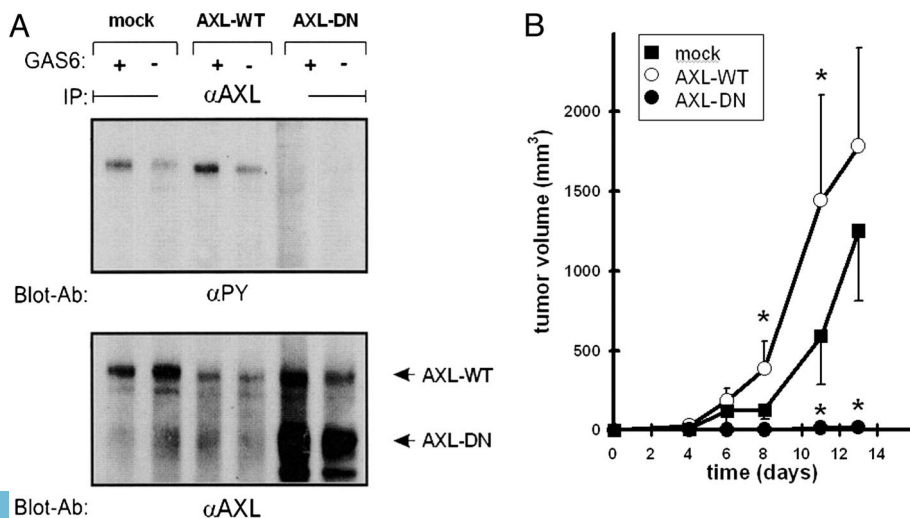


Fig. 2. Expression of a signaling-defective mutant form of Axl inhibits experimental tumor growth. (A) Western blot analysis of SF126 glioma cell clones expressing the control vector (mock), the wild-type form of Axl (AXL-WT), and a truncated dominant-negative mutant form of Axl (AXL-DN). Serum-depleted cells were left untreated (–) or treated with 200 μ g/ml Gas6 (+). Lysates were blotted with anti-phosphotyrosine serum (Upper) or an antibody directed against the extracellular domain of human Axl (Lower). (B) Analysis of tumor volume for SF126 experimental cell clones. Tumor cells were implanted s.c. into nude mice. The mean \pm SEM values are represented from eight animals per group. *, $P < 0.05$ vs. mock cells.

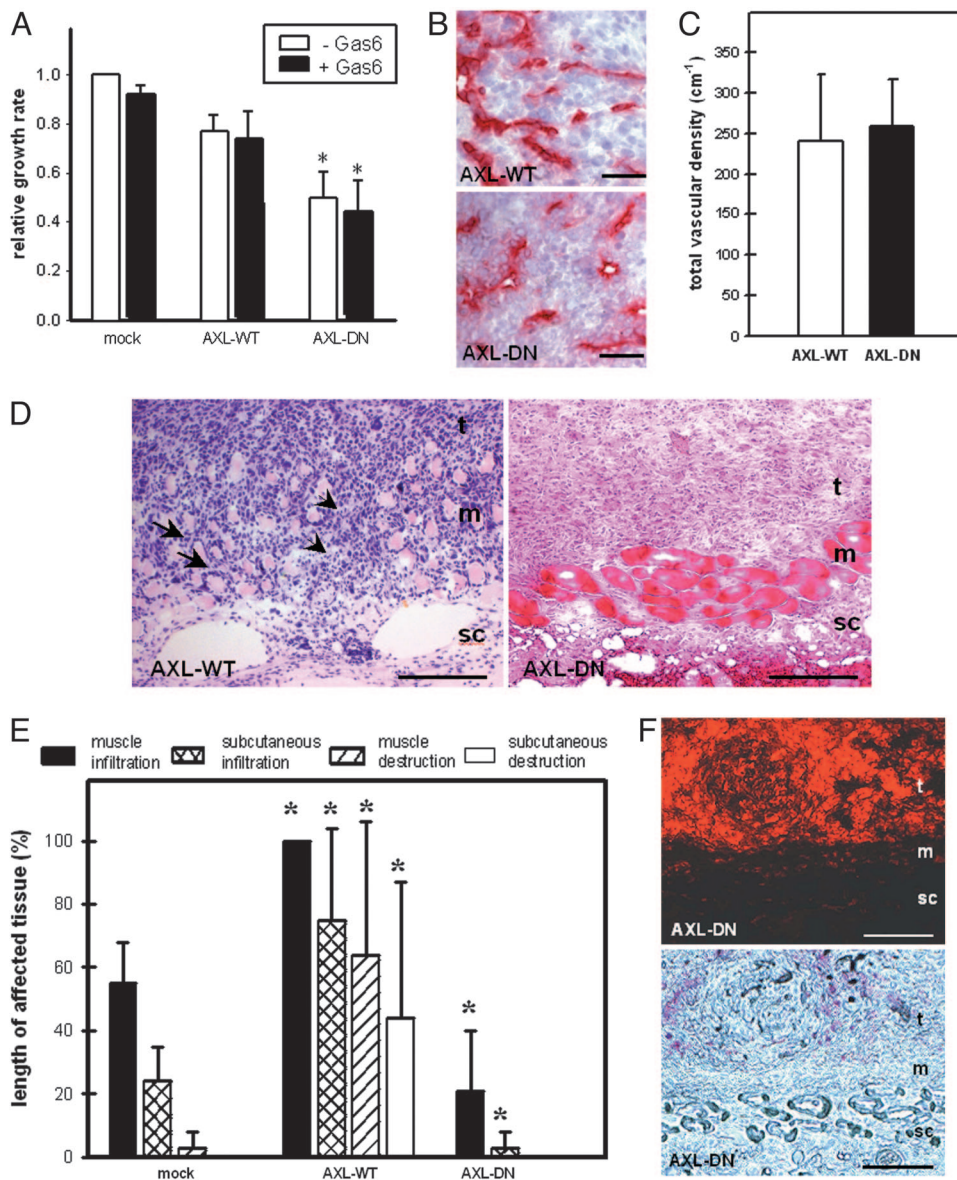


Fig. 3. Inhibition of Axl signaling suppresses diffuse-invasive tumor growth. (A) Proliferation assay of transfected cell clones. Cells were left untreated (–Gas6) or treated with 200 $\mu\text{g}/\text{ml}$ Gas6 (+Gas6). Analysis was performed after 48 h of culture. Growth rate is expressed in relation to unstimulated mock-transfected cells. Experiments were performed in triplicate. The mean \pm SD values are represented. *, $P < 0.05$ versus mock. (B and C) Assessment of vessel density in AXL-WT and AXL-DN xenografts after s.c. implantation. Analysis of tumor blood vessel density and morphology was assessed by immunohistochemistry for CD31 (B) and quantitatively by intravital fluorescence videomicroscopy after tumor implantation into the skinfold chamber preparation (C). The mean \pm SD values are represented from four animals per group. (Scale bars, 25 μm .) (D) Histomorphological images of AXL-WT tumors and AXL-DN tumors. Hematoxylin and eosin staining. Arrows indicate tumor cell invasion into the adjacent skin muscle layer resulting in displacement of the muscle tissue. Arrowheads indicate tumor cell invasion into the adjacent skin muscle layer resulting in destruction of the muscle tissue. t, tumor mass; m, skin muscle layer; sc, s.c. tissue. (Scale bars, 100 μm .) (E) Quantitative analysis of glioma cell invasion into adjacent tissue by mock, AXL-WT, and AXL-DN tumors. Linear analysis of the length of infiltrated and destroyed muscle and s.c. tissue is presented as percentage of the total cross-sectional length of tumor mass. The mean \pm SD values are represented. *, $P < 0.05$ versus mock tumors. (F) Fluorescence microscopy alone (Upper) and in combination with phase contrast (Lower) of AXL-DN tumor. Tumor cells were labeled with Dil before implantation. (Scale bars, 100 μm .) All specimens (B–F) were excised on day 21 after implantation into the dorsal skinfold chamber of nude mice. t, tumor mass; m, skin muscle layer; sc, s.c. tissue.

our model cell line (high Axl expression levels) (Fig. 1). Introduction of a dominant-negative mutant receptor is one strategy for studying the relevance of RTKs in cell function (23, 24). Thus, we introduced a truncated form of human Axl, lacking the intracellular RTK-bearing domain, into SF126 cells (AXL-DN). Cells transfected with an empty vector (mock) or a human wild-type form of Axl (AXL-WT) served as controls. Western blotting confirmed expression of the wild-type and truncated receptor in AXL-DN cell clones (Fig. 2A). Phosphotyrosine blotting for Axl after stimulation with Gas6 confirmed inhibition of Axl signal transduction (Fig. 2A). To determine whether Axl signaling is relevant for tumor growth, we generated s.c. xenografts in nude mice. When compared with control cells and AXL-WT cells, the tumorigenicity of AXL-DN cells was dramatically impaired (Fig. 2B).

Inhibition of Axl Signaling Suppresses Diffuse-Invasive Tumor Growth.

To further reveal the mechanisms underlying suppression of tumor growth by blocking of Axl signaling, we first assessed the proliferation characteristics of our cell clones. Overexpression of AXL-DN conferred a 50% and 30% growth disadvantage relative to mock and AXL-WT cells, respectively, confirming

Axl's role as a transforming/growth factor (Fig. 3A). This effect was independent of the presence of exogenous Gas6, confirming a high baseline activation of Axl. An additional mechanism by which Axl may influence tumor growth and expansion is its modulation of tumor blood vessel function (14, 18, 19, 25). To test this possibility, we implanted AXL-WT and AXL-DN cells into the dorsal skinfold chamber model of nude mice. This model allows for a noninvasive assessment of tumor growth, tumor angiogenesis, and tumor perfusion by intravital multifluorescence videomicroscopy (26). We could confirm the significance of Axl signaling for tumor growth: In comparison with AXL-WT tumors, expansion of AXL-DN tumors was again significantly suppressed (85% growth reduction versus AXL-WT tumors; $P < 0.05$). However, the analysis of tumor vessel density and tumor vessel diameter, by using CD31-immunohistochemistry (Fig. 3B) and intravital microscopy (Fig. 3C), failed to reveal an attenuated function of the tumor vasculature as an explanation for the reduced tumorigenesis of AXL-DN cells.

The most relevant clue of how Axl may additionally contribute to glioma biology was derived from the histomorphological analysis of the tumor specimens grown within the dorsal skinfold chamber. As

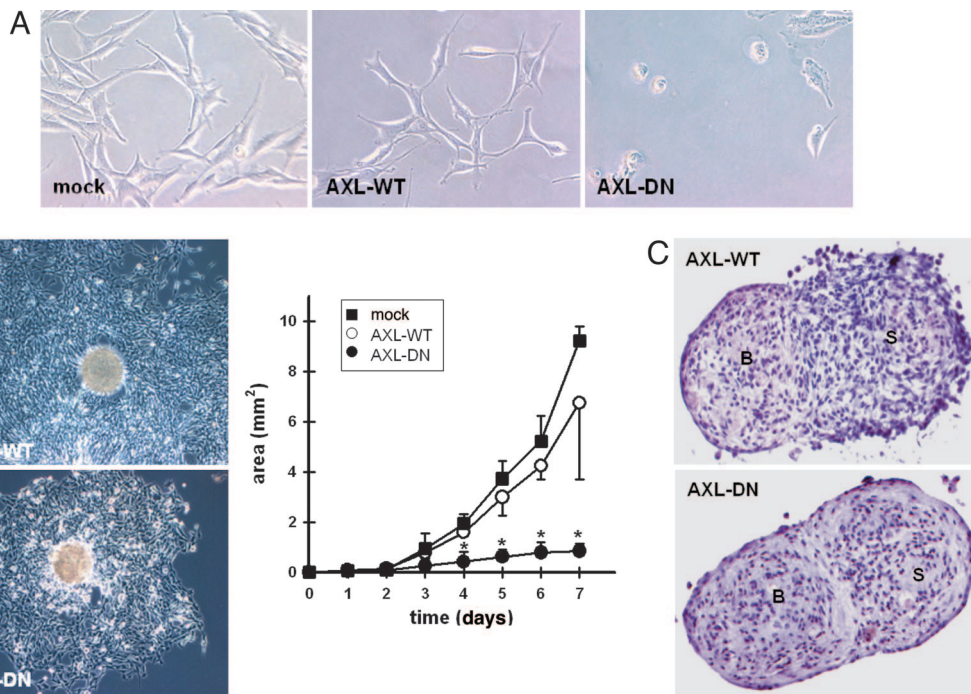


Fig. 4. *In vitro* characterization reveals role for Axl in mediating glioma cell migration and invasion. (A) Analysis of morphology and *in vitro* behavior of cell clones under nonconfluent conditions. (B) Migration assay with multicellular aggregates of transfected cell clones. Migratory activity of tumor cells is illustrated for AXL-WT and AXL-DN cells at 72 h after plating (Left) and is analyzed quantitatively over 7 days (Right). Area of migration was analyzed planimetrically by means of an image analysis system. Experiments were performed in triplicate. The mean \pm SD values are represented. *, $P < 0.05$ vs. mock-transfected cells. (C) Analysis of tumor cell invasion by 48-h confrontation of AXL-WT tumor cell spheroids (Upper) or AXL-DN tumor cell spheroids (Lower) with fetal rat brain cell aggregates. Note clear border between AXL-DN tumor cell spheroid and brain cell aggregate, whereas the AXL-WT spheroid has merged with the brain aggregate, indicating lack of invasiveness after inhibition of Axl signaling. B, brain cell aggregate; S, tumor spheroid. Experiments were performed in quadruplicate.

demonstrated in Fig. 3D, AXL-WT tumors were characterized by a massive invasion into the adjacent host tissue (i.e., skin muscle and s.c. tissue), whereas AXL-DN cells failed to invade the host tissue, resulting in a clear border between the tumor and the underlying host tissue. The quantitative analysis of tumor specimens at the tumor/adjacent tissue interface revealed that AXL-WT tumors invaded the adjacent tissue more aggressively than mock tumors (Fig. 3E). In contrast, AXL-DN tumors invaded the muscle and s.c. tissue to a significantly lesser extent than did mock and AXL-WT tumors (Fig. 3E). This apparent reduction of AXL-DN tumor invasion was further confirmed by fluorescence and phase-contrast microscopy (Fig. 3F).

Axl Mediates Glioma Cell Migration and Invasion. These results prompted us to assess the role of the Axl receptor for glioma cell migration in more detail, especially because the reduced tumor cell invasion *in vivo* could have been simply attributable to the reduced tumor cell load in AXL-DN tumors. In contrast, our *in vitro* assays clearly indicated that Axl is directly involved in tumor cell migration and invasion. Under regular culture conditions, AXL-DN cells partially detached and rounded up. Moreover, in contrast to mock or AXL-WT cells, AXL-DN cells displayed an attenuated locomotor activity with a reduced formation of filopodia and loss of cell-to-cell interactions (Fig. 4A). The notion that tumor cell motility is impaired in AXL-DN cells was further confirmed by an assay where glioma cell migration was assessed by plating tumor spheroids and measuring the area covered by tumor cells migrating from the originating spheroid over time (27). Although mock and AXL-WT cells migrated to a comparable extent, tumor cell migration was impaired in AXL-DN cells (Fig. 4B). Because cell migration is a prerequisite for tumor invasion, we addressed the invasiveness of our cell clones by confronting tumor spheroids with fetal rat brain cell aggregates (28). After 48 h of coculture, both

mock and AXL-WT cells had diffusely invaded the brain aggregate (Fig. 4C). In contrast, after the same time period, we could still observe a clear border between the AXL-DN tumor spheroid and the brain cell aggregate, indicating that these cells were unable to invade normal brain tissue (Fig. 4C).

Inhibition of Axl Signaling Prolongs Survival of Mice with Intracerebral Xenografts. Collectively, the histomorphology of the tumor xenografts and our *in vitro* results provided evidence that Axl is involved in multiple aspects of gliomagenesis. As a consequence, the Axl tyrosine kinase may represent a target for the treatment of malignant brain tumors. To test this hypothesis, AXL-WT and AXL-DN cells were orthotopically implanted, and their growth was assessed by using MRI. Ten days after implantation, MRI demonstrated that AXL-WT tumors had developed into large, space-occupying lesions (Fig. 5A). In contrast, in AXL-DN animals, contrast enhancement was detectable only along the needle tract (Fig. 5A). A volumetric analysis on day 10 after implantation confirmed this observation, with AXL-WT and AXL-DN tumors measuring $63 \pm 24 \text{ mm}^3$ and $<10 \text{ mm}^3$, respectively. This suppression of tumor growth translated into a marked prolongation of survival (Fig. 5B). The histomorphological analysis of the tumors revealed that overexpression of Axl in SF126 AXL-WT cells conferred an ability to invade the brain tissue diffusely, a growth behavior not displayed by parental SF126 cells (Fig. 5C and D). Note that the AXL-WT tumor depicted in Fig. 5D is of smaller size than the parental SF126 tumor in Fig. 5C but already invades the brain tissue, with cells infiltrating as individual cells and satellite tumors. In contrast, after the same time, AXL-DN tumors were smaller and lacked invasion of the brain parenchyma (Fig. 5D).

Discussion

The results of our analyses suggest a role for Axl in the biology of malignant brain tumors. Axl is overexpressed and activated in the

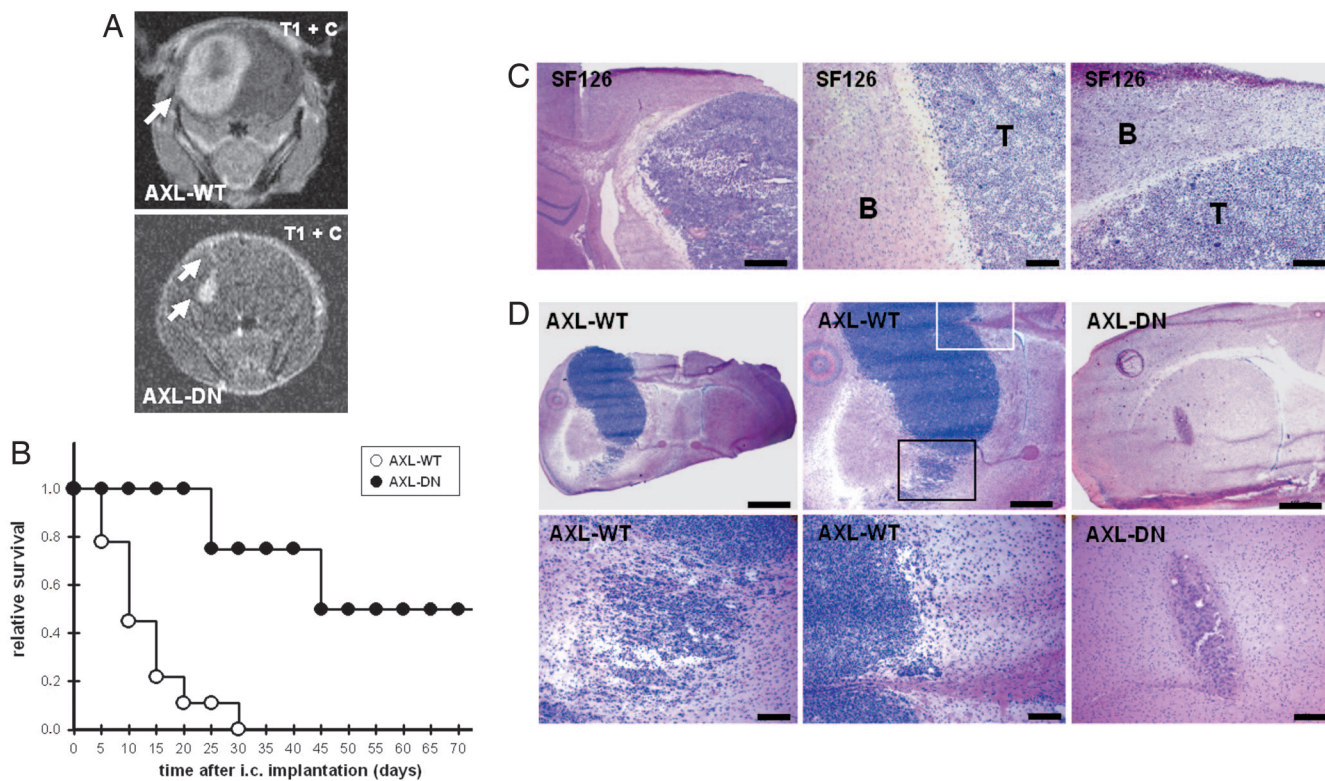


Fig. 5. Inhibition of Axl signaling prolongs survival after orthotopic implantation. (A) MRI of intracerebral tumor growth on day 10 after stereotactic implantation of AXL-WT and AXL-DN cells into the brains of nude mice. T1-imaging sequence after injection of gadolinium-DTPA. (B) Survival curves for nude mice after intracerebral implantation of AXL-WT cells ($n = 9$ animals) and AXL-DN cells ($n = 8$ animals). Animals were killed as soon as they developed neurological deficits or lost $>20\%$ of their initial body weight. (C) Histomorphology of parental SF126 tumors after intracerebral implantation demonstrating the typical growth behavior of this cell line in the CNS. SF126 cells grow primarily as a solid mass and show only little invasion. Note the clear-cut border between the tumor (T) and brain tissue (B). Hematoxylin and eosin staining. [Scale bars, $500\ \mu\text{m}$ (Left) and $100\ \mu\text{m}$ (Center and Right).] (D) Histomorphology of AXL-WT tumors and AXL-DN tumors on day 10 after intracerebral implantation. Whereas AXL-WT tumors had developed to large, space-occupying lesions with diffuse tumor cell infiltration into adjacent brain tissue (Left and Center), AXL-DN tumor cells had formed only small and well demarcated tumors (Right). Squares depict areas of AXL-WT tumor cell invasion highlighted at higher magnification. AXL-WT tumor cells invaded either diffusely into the brain tissue (black square and Left Lower) or along white-matter tracts, such as the corpus callosum (white square and Center Lower). Hematoxylin and eosin staining. [Scale bars, $1\ \text{mm}$ (Left Upper), $500\ \mu\text{m}$ (Center and Right Upper), and $100\ \mu\text{m}$ (Lower).]

majority of human glioma cell lines. Furthermore, Axl is expressed at high levels in glioblastoma multiforme, the most malignant form of brain tumor. Our analyses have disclosed that Axl, besides its known involvement in cell transformation and cell proliferation, also mediates migration and invasion of tumor cells. Finally, inhibition of Axl signaling has been demonstrated to suppress ectopic and orthotopic glioma growth and has resulted in a marked prolongation of survival. Thus, Axl represents a promising therapeutic target for interfering with these highly aggressive and, as yet, therapy-refractory, tumors. A similar role may be hypothesized for Axl in the biology of other human tumors (10–13).

To study the biological function of Axl in human glioma cells, we have inhibited its signaling function by expressing a truncated dominant-negative receptor mutant and analyzed the complex ability of the tumor cells to interact with each other and the matrix, in detail. Although we have tried to dissect the role of Axl for tumor biology in detail, we did not succeed in reducing the involvement of Axl in tumor cell biology to a single pathological process. In fact, inhibition of Axl signaling to some extent negatively interfered with tumor cell proliferation, cell–cell interactions, and cell migration and invasion, suggesting multiple roles for Axl in tumorigenesis. Nevertheless, the most relevant observation that we made was that inhibition of Axl signaling almost completely suppresses the cells' ability to migrate into and invade healthy host tissue. It is noteworthy that the effect of

Axl expression on tumor cell invasion varied between the s.c. and intracerebral implantation site. In the s.c. implantation site, the parental SF126 cells already display a strong invasion into the adjacent tissue, which can be increased by further expression of Axl and can be blocked by inhibition of Axl signaling. In contrast, in the CNS, the parental SF126 cells grow as a solid mass and invade only a little into the brain parenchyma, a phenomenon that most glioma cell lines have in common when xenografted into the brain. Only after further expression of Axl, do the cells invade the cerebral tissue, whereas inhibition of Axl signaling primarily affects glioma expansion. These observations clearly suggest that the role of Axl in gliomagenesis may, in part, depend on the host microenvironment.

That Gas6/Axl interactions may be involved in directed cell migration has been suggested for vascular smooth muscle cells in the context of remodeling of the vessel wall after vascular injury (29) and for endothelial cells during tumor angiogenesis (25). By using an *in vitro* chemotaxis assay, the ectopic expression of Axl in vascular smooth muscle cells has been shown to increase the Gas6-induced migratory response, a phenomenon that depends on an intact, signaling-competent Axl tyrosine kinase. Investigations of the downstream signaling pathways have demonstrated a role for phosphatidylinositol 3-kinase and phospholipase C- γ in Gas6-induced migration of vascular smooth muscle cells (29).

Because of their relevance in tumor biology, RTKs are being actively pursued as therapeutic targets (30, 31). Trastuzumab, a monoclonal antibody against the RTK HER2/neu (32), is now in clinical use and has been shown to be effective in the treatment of HER2-positive breast cancer. Inhibition of Axl signaling by transfer of genes encoding a mutant receptor or by generation of inhibitory-specific monoclonal antibodies or small molecule kinase inhibitors may now be realistic strategies for interfering with the progression of malignant brain tumors to prolong survival of patients suffering from this devastating disease.

Materials and Methods

Cell Lines. Cell lines and culture conditions are described in *Supporting Materials and Methods*, which is published as supporting information on the PNAS web site.

cDNA Array Preparations and Hybridizations. Gene expression was analyzed by hybridization of nylon filter arrays with radioactive targets (cDNA) (see *Supporting Materials and Methods*).

RNA Analysis by Northern Blot. We used the standard protocol of Northern blot analysis for detection of the expression of Axl and Gas6 genes in human glioma cell lines. The loading RNA samples were verified by rehybridization of filters with human β -actin probe.

Immunoprecipitation and Western Blotting. Axl-specific antibodies were generated and phosphotyrosine blotting was performed as described in *Supporting Materials and Methods*.

Generation of Expression Constructs and Stable Cell Lines. Axl wild type (AXL-WT) and a dominant-negative variant (AXL-DN) were expressed in SF126 cells by using the retroviral factor pLXSN (see *Supporting Materials and Methods*).

In Vitro Biological Assays. In order to study the role of Axl for tumor cell biology, *in vitro* proliferation, migration, and invasion assays were performed (see *Supporting Materials and Methods*).

Experimental Tumor Models. Glioma xenografts were grown s.c. and intracerebrally. For intravital microscopic analyses, glioma cells were implanted into the dorsal skinfold chamber model (24) (see *Supporting Materials and Methods*). The volumetric analysis of the tumors is outlined in *Supporting Materials and Methods*.

Visualization of Brain Tumors. Intravital epifluorescence videomicroscopy was performed over 21 days after implantation as described in ref. 33. Contrast-enhanced MRI was performed 10 days after implantation. MRI was performed on a clinical 1.5 T MR system (Symphony; Siemens, Erlangen, Germany) using a dedicated animal in-house-manufactured volume coil.

Experimental and Human Tumor Specimens. Upon completion of experiments, the glioma-containing dorsal skinfold chamber preparations and brains were dissected free. Human glioma specimens were obtained from surgical tumor resections in accordance with the local Ethics Committee. The histoanalyses are detailed in *Supporting Materials and Methods*.

Statistics. For analysis of differences between the groups, one-way ANOVA, followed by the appropriate post hoc test for individual comparisons between the groups, was performed. Results with $P < 0.05$ were considered significant.

We thank S. Mohr and V. Powajbo for excellent technical assistance, Dr. Yuri Cheburkin (Max Planck Institute for Biochemistry) for the array analysis contribution, and Dr. Takako Sasaki (Max Planck Institute for Biochemistry) for the purification of GAS6 used in our study. This study was supported by grants from the German Research Foundation (DFG SPP1190: VA151/6-1) and the 6th framework of the European Union (STROMA).

- DeAngelis, L. M. (2001) *N. Engl. J. Med.* **344**, 114–123.
- Stupp, R., Mason, W. P., van den Bent, M. J., Weller, M., Fisher, B., Taphoorn, M. J., Belanger, K., Brandes, A. A., Marosi, C., Bogdahn, U., et al. (2005) *N. Engl. J. Med.* **352**, 987–996.
- Lefranc, F., Brothi, J. & Kiss, R. (2005) *J. Clin. Oncol.* **23**, 2411–2422.
- Ullrich, A. & Schlessinger, J. (1990) *Cell* **61**, 203–212.
- Janssen, J. W., Schulz, A. S., Steenvoorden, A. C., Schmidberger, M., Strehl, S., Ambros, P. F. & Bartram, C. R. (1991) *Oncogene* **6**, 2113–2120.
- O'Bryan, J. P., Frye, R. A., Cogswell, P. C., Neubauer, A., Kitch, B., Prokop, C., Espinosa, R., III, Le Beau, M. M., Earp, H. S. & Liu, E. T. (1991) *Mol. Cell. Biol.* **11**, 5016–5031.
- Faust, M., Ebensperger, C., Schulz, A. S., Schleithoff, L., Hameister, H., Bartram, C. R. & Janssen, J. W. (1992) *Oncogene* **7**, 1287–1293.
- Prieto, A. L., Weber, J. L. & Lai, C. (2000) *J. Comp. Neurol.* **425**, 295–314.
- Funakoshi, H., Yonemasu, T., Nakano, T., Matumoto, K. & Nakamura, T. (2002) *J. Neurosci. Res.* **68**, 150–160.
- Meric, F., Lee, W. P., Sahin, A., Zhang, H., Kung, H. J. & Hung, M. C. (2002) *Clin. Cancer Res.* **8**, 361–367.
- Wimmel, A., Glitz, D., Kraus, A., Roeder, J. & Schuermann, M. (2001) *Eur. J. Cancer* **37**, 2264–2274.
- Challier, C., Uphoff, C. C., Janssen, J. W. & Drexler, H. G. (1996) *Leukemia* **10**, 781–787.
- Craven, R. J., Xu, L. H., Weiner, T. M., Fridell, Y. W., Dent, G. A., Srivastava, S., Varnum, B., Liu, E. T. & Cance, W. G. (1995) *Int. J. Cancer* **60**, 791–797.
- Stitt, T. N., Conn, G., Gore, M., Lai, C., Bruno, J., Radziejewski, C., Mattsson, K., Fisher, J., Gies, D. R., Jones, P. F., et al. (1995) *Cell* **80**, 661–670.
- Bellosta, P., Costa, M., Lin, D. A. & Basilico, C. (1995) *Mol. Cell. Biol.* **15**, 614–625.
- Bellosta, P., Zhang, Q., Goff, S. P. & Basilico, C. (1997) *Oncogene* **15**, 2387–2397.
- van Ginkel, P. R., Gee, R. L., Shearer, R. L., Subramanian, L., Walker, T. M., Albert, D. M., Meisner, L. F., Varnum, B. C. & Polans, A. S. (2004) *Cancer Res.* **64**, 128–134.
- Fridell, Y. W., Villa, J., Jr., Attar, E. C. & Liu, E. T. (1998) *J. Biol. Chem.* **273**, 7123–7126.
- Galliechio, M., Mitola, S., Valdembrì, D., Fantozzi, R., Varnum, B., Avanzi, G. C. & Bussolino, F. (2005) *Blood* **105**, 1970–1976.
- Bange, J., Precht, D., Cheburkin, Y., Specht, K., Harbeck, N., Schmitt, M., Knyazeva, T., Müller, S., Gartner, S., Sures, I., et al. (2002) *Cancer Res.* **62**, 840–847.
- Dirks, W., Rome, D., Ringel, F., Jäger, K., MacLeod, R. A. & Drexler, H. G. (1999) *Leuk. Res.* **23**, 643–651.
- O'Bryan, J. P., Fridell, Y. W., Koski, R., Varnum, B. & Liu, E. T. (1995) *J. Biol. Chem.* **270**, 551–557.
- Millauer, B., Shawver, L. K., Plate, K. H., Risau, W. & Ullrich, A. (1994) *Nature* **367**, 576–579.
- Strawn, L. M., Mann, E., Elliger, S. S., Chu, L. M., Germain, L. L., Niederfellner, G., Ullrich, A. & Shawver, L. K. (1994) *J. Biol. Chem.* **269**, 21215–21222.
- Holland, S. J., Powell, M. J., Franci, C., Chan, E. W., Friera, A. M., Atchison, R. E., McLaughlin, J., Swift, S. E., Pali, E. S., Yam, G., et al. (2005) *Cancer Res.* **65**, 9294–9303.
- Vajkoczy, P., Farhadi, M., Gaumann, A., Heidenreich, R., Erber, R., Wunder, A., Tonn, J. C., Menger, M. D. & Breier, G. (2002) *J. Clin. Invest.* **109**, 777–785.
- Vajkoczy, P., Menger, M. D., Goldbrunner, R., Ge, S., Fong, T. A., Vollmar, B., Schilling, L., Ullrich, A., Hirth, K. P., et al. (2000) *Int. J. Cancer* **87**, 261–268.
- Bjerkvig, R., Laerum, O. D. & Mella, O. (1986) *Cancer Res.* **46**, 4071–4079.
- Melaragno, M. G., Fridell, Y. W. & Berk, B. C. (1999) *Trends Cardiovasc. Med.* **9**, 250–253.
- Gschwind, A., Fischer, O. M. & Ullrich, A. (2004) *Nat. Rev. Cancer* **4**, 361–370.
- Shawver, L. K., Slamon, D. & Ullrich, A. (2002) *Cancer Cell* **1**, 117–123.
- Hudziak, R. M., Lewis, G. D., Winget, M., Fendly, B. M., Shepard, H. M. & Ullrich, A. (1989) *Mol. Cell. Biol.* **9**, 1165–1172.
- Vajkoczy, P., Schilling, L., Ullrich, A., Schmiedek, P. & Menger, M. D. (1998) *J. Cereb. Blood Flow Metab.* **18**, 510–520.